ELSEVIER

Contents lists available at ScienceDirect

Additive Manufacturing Letters

journal homepage: www.elsevier.com/locate/addlet



Short Communication

Conformal 3D printing of a polymeric tactile sensor

Omar Faruk Emon^a, Faez Alkadi^b, Mazen Kiki^c, Jae-Won Choi^{c,*}

- a Department of Mechanical and Industrial Engineering, University of New Haven, 300 Boston Post Rd, West Haven, CT 06516, United States
- ^b Department of Mechanical Engineering, Jazan University, Jazan 45142, Saudi Arabia
- ^c Department of Mechanical Engineering, The University of Akron, 244 Sumner Street, Akron, OH 44325, United States



Keywords: Conformal 3d printing Stretchable electronics Ionic liquid Soft pressure sensor Curvilinear printing Curved sensor

ABSTRACT

Conventional additive manufacturing processes are generally inadequate for printing electronics on a curved surface. When printing a curved functional structure, the typical way of generating the extrusion path only in a horizontal plane could cause various issues such as impreciseness and disconnect in the printed part. In this work, conformal 3D printing of a soft tactile sensor is presented in which curvilinear extrusion paths were generated for the printing of a curved sensor. An extrusion-based multi-material direct printing system was employed to print the sensor, and ultraviolet light was used to polymerize the printed layers. An ionic liquid-based pressure-sensitive polymer membrane, carbon nanotube-based conductive electrodes, and a soft polymeric insulation layer were conformally 3D printed to fabricate the curved sensor on a fingertip model. The conformally printed sensor was evaluated under different conditions. Sensors 3D-printed using conformal and planar slicing processes were compared to investigate the effect of curvilinear slicing on the printed parts. The results show that conformal 3D printing is able to overcome the fabrication limitations of conventional planar processing while also retaining the functionality of the printed structures.

1. Introduction

Additive manufacturing (AM) or three-dimensional (3D) printing has advanced significantly in the past decade. On one hand, newer volumetric processes [1] and improvements to conventional AM [2] have been proposed. On the other hand, AM has been employed in functional part fabrication by widening the selection of materials for printing [3-5]. The manufacturing and design flexibility provided by AM makes it a suitable fabrication technique for custom electronics such as sensors and actuators [6,7]. In particular, 3D printed soft sensors are opening newer avenues in the area of robotics [8,9], prosthetics [10,11], bioapplications [12,13], and wearable electronics [14,15]. Soft and flexible tactile/pressure sensors provide many benefits over rigid sensors, especially in robotics and wearable electronics, as soft sensors can flex, bend, and absorb shocks [16]. Various printing processes have been reported for soft sensor fabrication such as direct extrusion [17], stereolithography [18], and jetting [19]. While 3D printing enables the customization of designs and materials, soft sensors provide mechanical pliability. Therefore, printed soft electronics has become an area of interest for a wide range of applications [20-22].

Soft polymers have been widely utilized for printed electronics [23,24]. Various piezoresistive [25] and piezoelectric [26] polymers and polymer composites have been proposed for sensors and actuators

* Corresponding author.

E-mail address: jchoi1@uakron.edu (J.-W. Choi).

[27]. Carbon nanotube (CNT)-based polymer composites are commonly used for printing flexible and stretchable conductive wires or electrodes [28,29]. Recently, ionic liquid (IL) has been incorporated with polymers to develop a solid-state pressure-sensitive IL/polymer membrane [30]. The IL and CNT-based polymer composites are very suitable options for extrusion-based direct printing, as they can be polymerized immediately. These materials are modified and applied to the direct-print photopolymerization process to facilitate the 3D printing of stretchable pressure sensors [17]. The incorporation of IL introduces more controllable parameters to the pressure sensor that allow for adjusting sensor properties according to the application. In addition, the IL-based polymer network is an electrochemically stable and green alternative to many printable materials for electronics [31]. Although several studies were conducted on printed flat sensors [32], there are opportunities for research on printed non-flat sensors. In this work, an IL-based curved polymeric tactile sensor was 3D printed via an extrusion-based directprint photopolymerization system.

In general, conventional additive manufacturing involves the addition of horizontal layers of material to print a 3D structure. The extrusion or motion is limited to two-dimensional (2D) or X-Y movement, and a single line or a layer will typically show no 3D (X-Y-Z) movement. This process is referred to as *planar printing*, and it is useful for printing an object with a simple geometry on a flat surface. However, for a curved fixture on a non-flat substrate, planar printing can have several drawbacks. To show the limitations of planar printing, an example of an electrode on a fingertip is shown in Fig. 1(a). The electrode follows the curvature of the fingertip. In conventional planar printing,

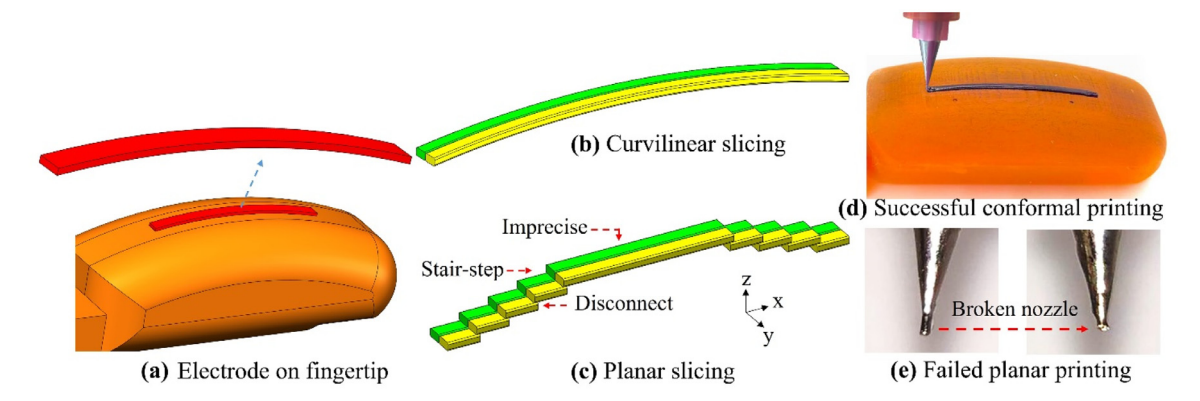


Fig. 1. Limitations of planar slicing: (a) a curved electrode to be printed on a non-flat substrate; (b) curvilinear extrusion path; (c) planar extrusion path; (d) successful conformal printing of the electrode on a fingertip; (e) broken print nozzle tip when printing a planar-sliced electrode.

the 3D model of the electrode is sliced to generate 2D layers and extrusion paths as shown in Fig. 1(c). It is evident from Fig 1(c) that planar slicing is imprecise and would create a staircase effect, in which the layer marks are visible on the surface of the printed part. More importantly, because of the small overlap between layers, a disconnect between layers can be created that may impact the electrical conductivity of the electrode. When an attempt was made to print an electrode on a fingertip model using planar 3D printing, it completely failed to print the electrode. Because of the small 2D motion, the print nozzle could not decelerate quickly enough; instead, it hit the rigid fingertip model (due to its curvature), and the nozzle tip was broken, as shown on the right-hand side in Fig. 1(e). Next, for the same model, a curvilinear extrusion path was created following the curvature of the fingertip, as shown in Fig. 1(b). Using this path, the extrusion is no longer limited to a horizontal plane, as it involves a 3D movement. Using this process of printing, which is referred to as conformal printing, the electrode was successfully printed on the fingertip model as shown in Fig. 1(d). Moreover, conformal 3D printing would take less time to print curved structures as it does not involve as many start-stops as planar printing. This work describes conformal 3D printing of a curved and soft tactile

2. Materials and methods

2.1. Sensor design and materials for fabrication

The proposed sensor is a soft pressure/tactile sensor designed to be printed on a curved surface (i.e., a fingertip), and the curvature of the sensor is the same as that of the fingertip surface. The sensor design uses multiple layers and materials, in which a pressure-sensitive IL/polymer membrane is sandwiched between CNT/polymer-based electrodes, as shown in Fig. 2. One electrode on each side of an IL/polymer membrane creates a single sensitive zone, which is referred to as a taxel. An array of taxels can be created with multiple electrodes on different sides of the IL/polymer membrane. The top layer of the sensor is an insulation layer that isolates the sensor from the external environment. All layers of the sensor are soft, stretchable, and polymeric, and any deformation or strain on the IL/polymer network will result in a change in the electrical resistance of the layer. As illustrated in Fig. 2, a potential divider with an external power supply (V_{in}) and resistor (R_{ex}) can be used to determine the sensor response in terms of the voltage output (V_{out}) . An applied force on the taxel changes the distance between electrodes and subsequently alters the IL/polymer resistance, which eventually causes a deviation in the V_{out} .

A commercially available photocurable resin, TangoPlus FLX930 (Stratasys, Eden Prairie, Minn., USA), was used as the base polymer for the sensor fabrication. TangoPlus is an acrylate-based flexible and stretchable photopolymer. In the prepolymer phase, it is a low viscos-

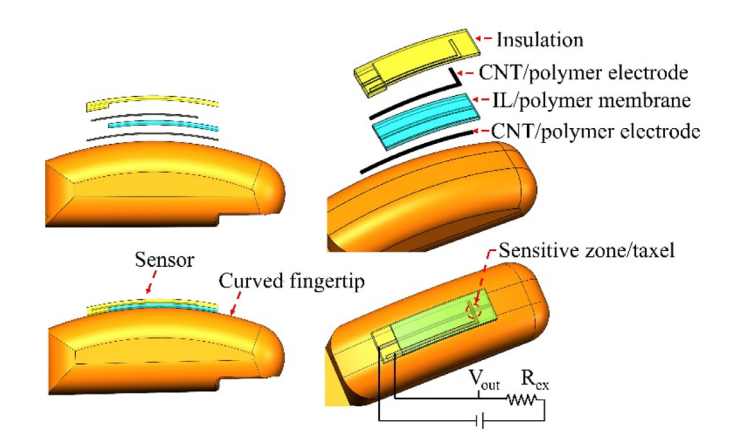


Fig. 2. Schematic of a curved pressure sensor on a fingertip, its multiple layers with different materials, and the simplified wiring diagram for the sensor.

ity liquid that polymerizes under ultraviolet (UV) light. However, in this study, the prepolymer TangoPlus was mixed with 10 wt.% CAB-O-SIL® M5 fumed silica (Cabot Corporation, Billerica, Mass., USA) to achieve rheological properties for extrusion-based direct printing so that the printed line holds its shape and can maintain a consistent linewidth at 15 mm/s travel speed after printing. The fumed silica (FS) introduces shear-thinning properties into the prepolymer paste, which helps in retaining the filament shape after extrusion. This paste-like prepolymer was used to print the top insulation layer of the sensor. For the pressuresensitive intermediate layer, 1 wt.% IL, 1-ethyl-3-methylimidazolium tetrafluoroborate (EMIMBF4; obtained from Sigma-Aldrich, Milwaukee, Wisc., USA), was mixed with the TangoPlus/FS. The electrode material was prepared by dispersing 5 wt.% CNT into TangoPlus/FS. Uniform dispersion of CNT was accomplished by using a surfactant (Triton X100, obtained from Sigma-Aldrich) and sonication in the presence of the solvent dimethylformamide, which was also obtained from Sigma-Aldrich

2.2. Multi-Material direct-print photopolymerization system

A custom-built extrusion-based direct printing system with multimaterial printability has been developed for sensor fabrication [17]. As shown in Fig. 3, the system consists of three motorized stages, dispensing units with multiple extruders, air-based pressure controllers, a UV lamp, and an optical cable. The extruder syringes are capable of extruding viscous paste with a variety of nozzle diameters ranging from 50 μ m to 500 μ m. In addition to the ability to print with multiple materials, the system also provides options for adjusting the dispensing pressure and

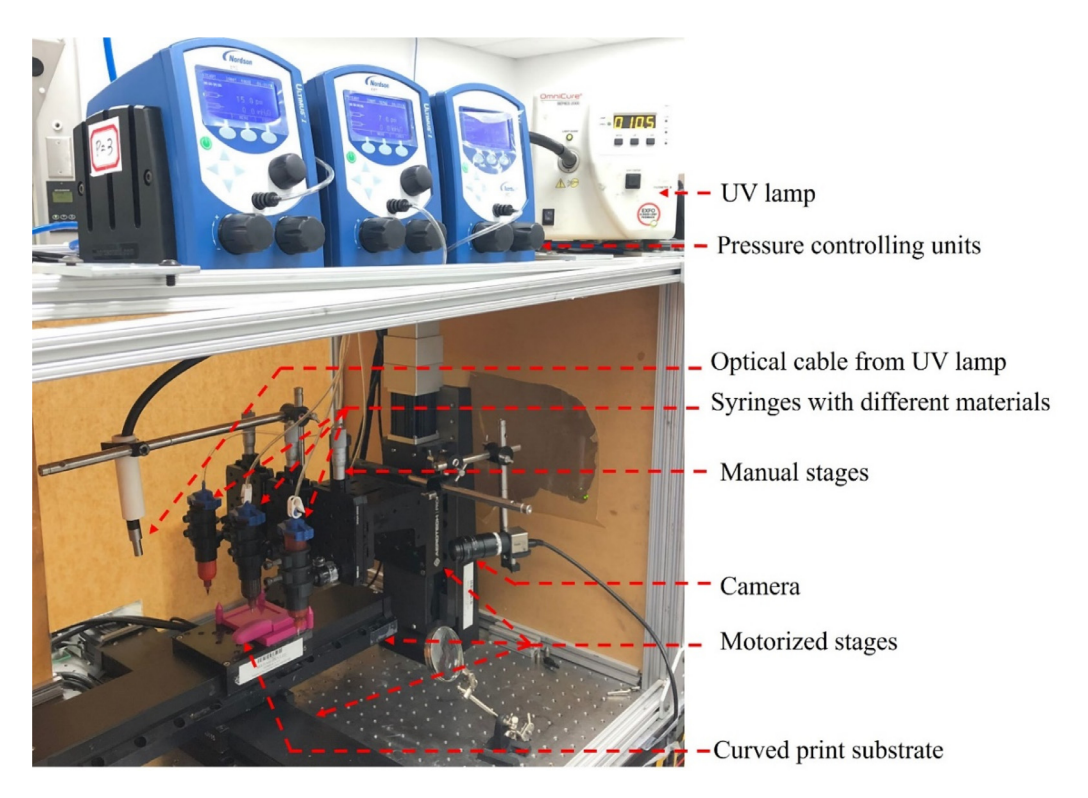


Fig. 3. Multi-material extrusion-based direct-print photopolymerization system.

travel speed for different materials. A reference base was 3D printed using a commercial printer that can hold different print substrates. A high-resolution camera and adjustable manual stages were used to home the extruders with respect to the reference base. An enclosure was built to restrict the UV light within the chamber, and each printed layer was photopolymerized using UV light.

2.3. Curvilinear extrusion path for conformal printing

The goal of this work is to conformally 3D print a sensor on a curved fingertip surface. The curved sensor was designed using the computeraided design (CAD) software SOLIDWORKS from an existing CAD model of the fingertip to enable the sensor to follow the curvature of the finger. Because the sensor design uses three different materials, the sensor CAD model was separated into three parts (one for each material), and a curvilinear extrusion path was generated for conformal 3D printing of a single layer that may include multiple materials [2]. All CAD models were converted into standard triangle language (STL) files that provide the surface geometry of the 3D models. First, a curved slicer surface was extracted from the fingertip model (Fig. 4(b)). Next, to generate the curvilinear extrusion path of the first layer, all three parts of the sensor were sliced using the curved slicer from the fingertip. Initially, the print-perimeters for different parts were created from the intersection of the slicer and the sensor parts. Finally, a 2D fill pattern was projected onto the curved and sliced surface within that perimeter to generate the curvilinear extrusion path for different portions of the first layer. This process was repeated with different slicing heights to obtain the extrusion path for the subsequent layers until no intersection between the slicer surface and the sensor 3D model remained. The programming and numeric computing platform MATLAB was utilized to employ this algorithm using the surface geometry of the slicer and the sensor model. Figs. 4(c)-4(h) show the curvilinear extrusion paths for six different layers. These extrusion paths were used to develop the G-code for motion and extrusion control in the direct-print system. Electrical wires were pierced through the sensor to connect with

the electrodes. As the IL-wire connection may interfere with the sensor signal, the wiring zone (at the bottom) of the sensor was maintained IL-free. Therefore, the first layer includes insulation material as shown in Fig. 4(c).

2.4. Experimental setup for sensor tests

The conformally 3D-printed sensor was evaluated under different conditions. A compressive force was first applied to the taxel to check the sensor response. The applied force was measured using an M5-5 force gage (Mark-10 Corporation, Copiague, N.Y., USA) and the sensor signal output was measured in terms of voltage using a BNC-2090A data acquisition system from National Instruments (Austin, Texas, USA). The sensor was connected in a potential divider circuit where the supplied voltage was 24 V and the external resistor was 20 M Ω (Fig. 2(c)). An A-LSQ075A-E01 motorized stage (Zaber Technologies, Vancouver, B.C., Canada) was used to apply force on the sensor. The taxel on the printed sensor had an inclination angle with respect to the horizontal plane. To apply a normal compressive force on the taxel, the fingertip was rotated so that the inclination was canceled out. From the CAD model, the inclination angle with the horizontal plane at the taxel was measured as 8.04° (Fig. 5). Therefore, the fingertip was placed on a rotation stage, and it was rotated 8° to apply a normal compressive force on the taxel. All devices were interfaced to MATLAB, which was used to control them and to collect data. A probe with a diameter of 3 mm was attached to the force gage to apply force on the taxel.

3. Results

3.1. Conformal printing of CNT-based electrodes

First, the effect of conformal 3D printing was investigated using the CNT/polymer conductive ink. Three different print processes were attempted with a constant geometry: Method A in-

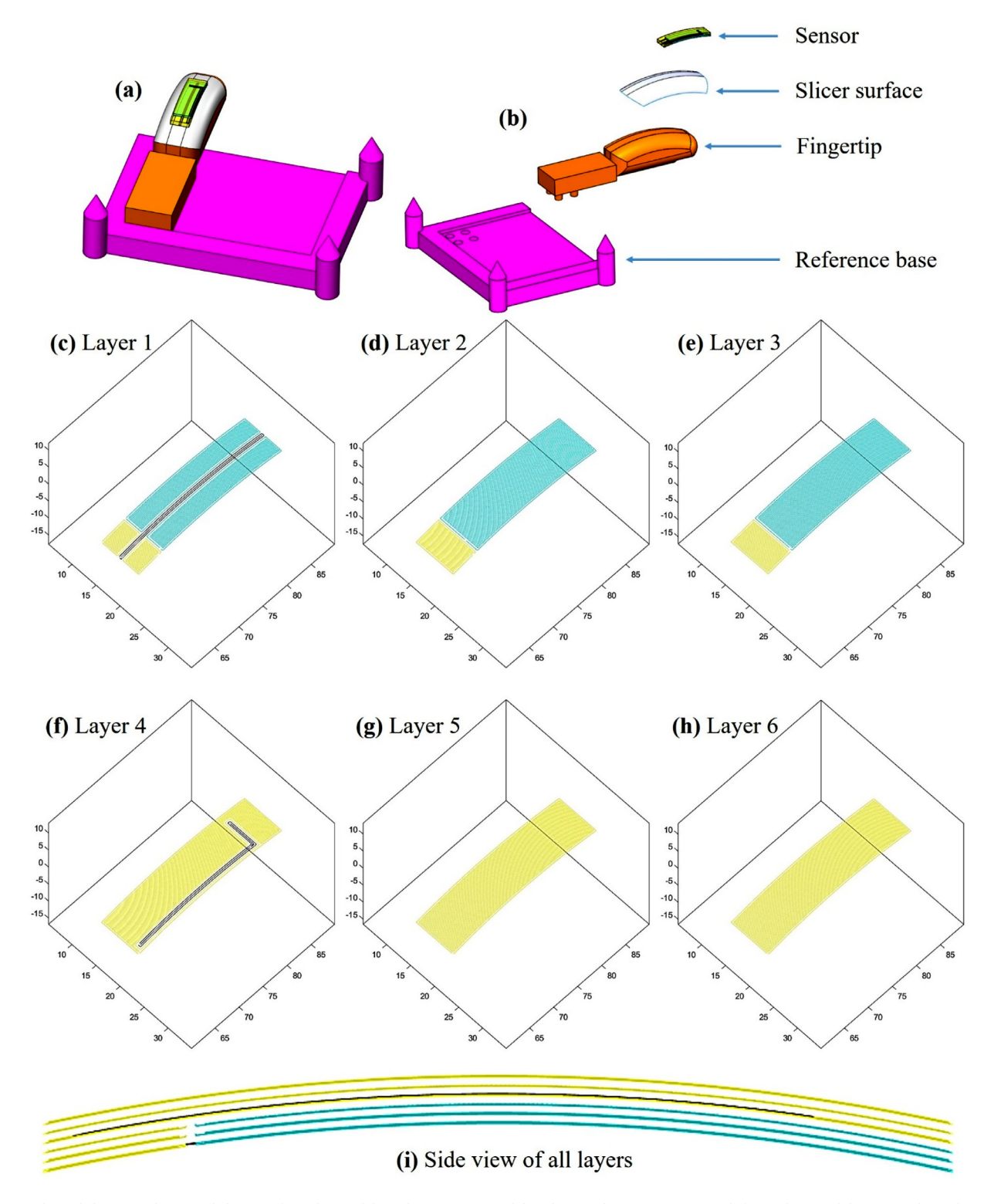


Fig. 4. Conformal slicing: (a-b) curved slicer surface obtained from fingertip 3D model; (c-h) curvilinear extrusion path for six layers of the sensor through conformal slicing; and (i) side view of curvilinear extrusion path for all layers.

volved planar printing on a flat surface, Method B involved planar printing on a curved surface, and Method C involved conformal printing on a curved surface. While Methods A and C were successful, planar printing on a curved surface (Method B) was a failed attempt. Multiple extrusion nozzles broke as they made contact with the curved substrate within a small planar motion. Fig. 6(a) shows planar and conformal 3D printing of CNT-based lines. The CAD model

was designed with a line of 0.8 mm in width. The printed line width for both conformal and planar printing was around 0.8 mm before curing, as shown in Fig. 6(b). No significant difference in linewidth was noticed between before and after curing/polymerization. The resistivities of the printed lines were also measured; as can be noticed from Fig. 6(c), the difference in resistivity between planar and conformal printing was not substantial.

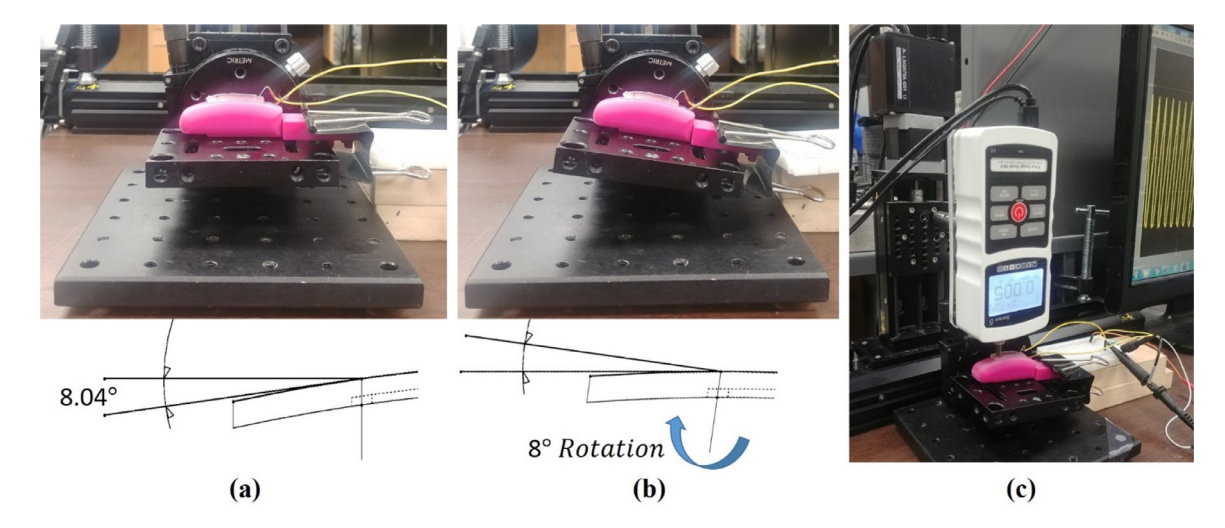


Fig. 5. Conformally printed sensor test setup: (a) fingertip with the sensor mounted on rotation stage; (b) stage rotated 8° to apply force normally on the taxel; and (c) experimental setup with a force gage, motorized stage, and data acquisition system.

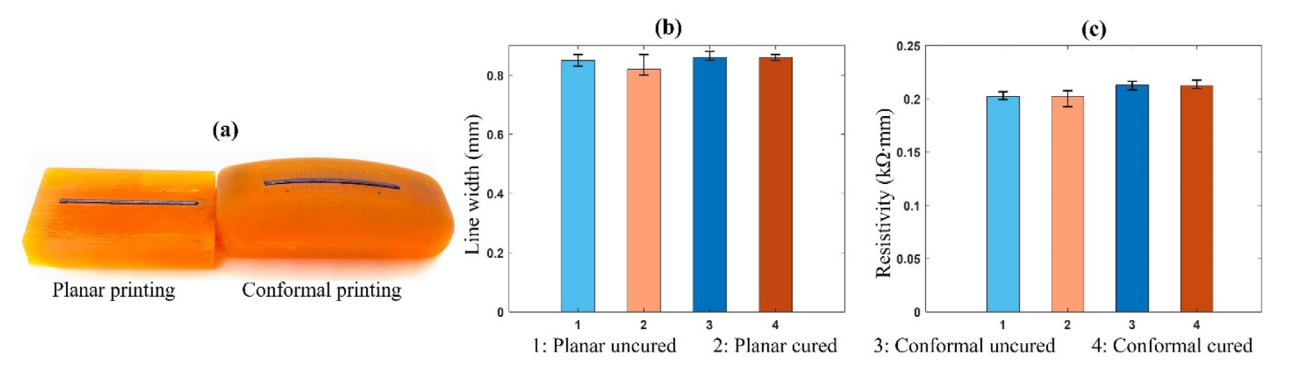


Fig. 6. Printed CNT-based electrode: (a) planar printing on a flat surface and conformal printing on a curved surface; (b) Line width of the printed line before and after curing; (c) electrical resistivity before and after curing.

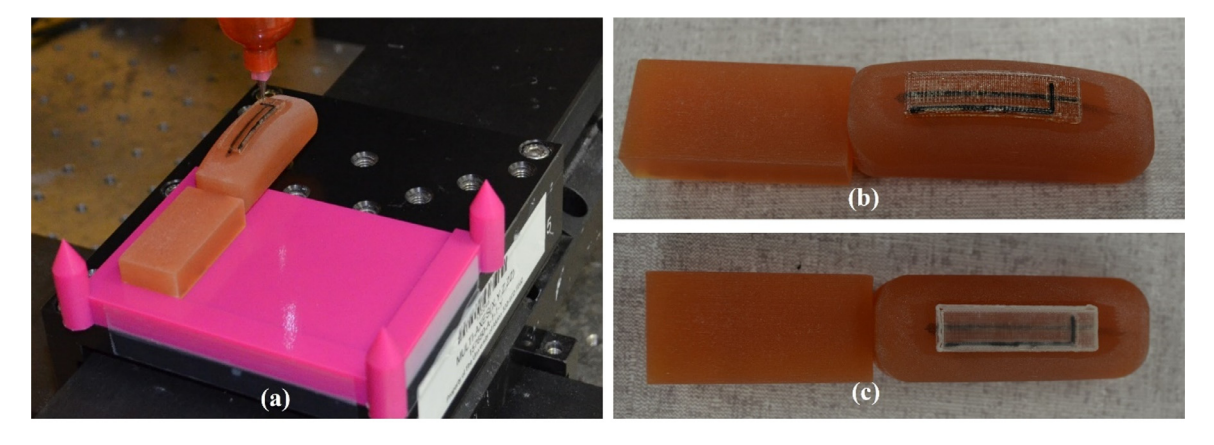


Fig. 7. Conformally printed curved sensor: (a) conformal 3D printing process; (b) uncured sensor; (c) photopolymerized sensor.

3.2. Conformal 3D printing of the sensor

For conformal 3D printing of the sensor, the three syringes in the direct-print system were filled with three different materials: IL/prepolymer, insulation prepolymer, and CNT/prepolymer. A fingertip model was 3D printed using a commercial polyjet 3D printer (Stratasys, Eden Prairie, Minn., USA). The printed fingertip was secured to the reference base with the help of LEGO®-like studs. The sensor was printed using nozzle diameters of 335 μ m, a layer height of 300 μ m, and a travel speed of 15 mm/s. The printed sensor was approximately

1.8 mm thick with a 1-mm \times 1-mm taxel. Fig. 7(a) shows the sensor being conformally 3D printed, while Fig. 7(b) and 7(c) show the uncured and cured/polymerized sensors, respectively. Each layer was photopolymerized with UV light after printing.

Fig. 8 presents the results for different sensor tests. First, the sensor was subjected to a fixed strain of 60% for multiple cycles at a probe speed of 0.1 mm/s. Fig. 8(a) shows the applied force and relative change in voltage output from the sensor system. While loading, the sensor response was nearly instantaneous (a delay of less than 10 ms) with the force. However, a delay was observed in the unloading curve. The un-

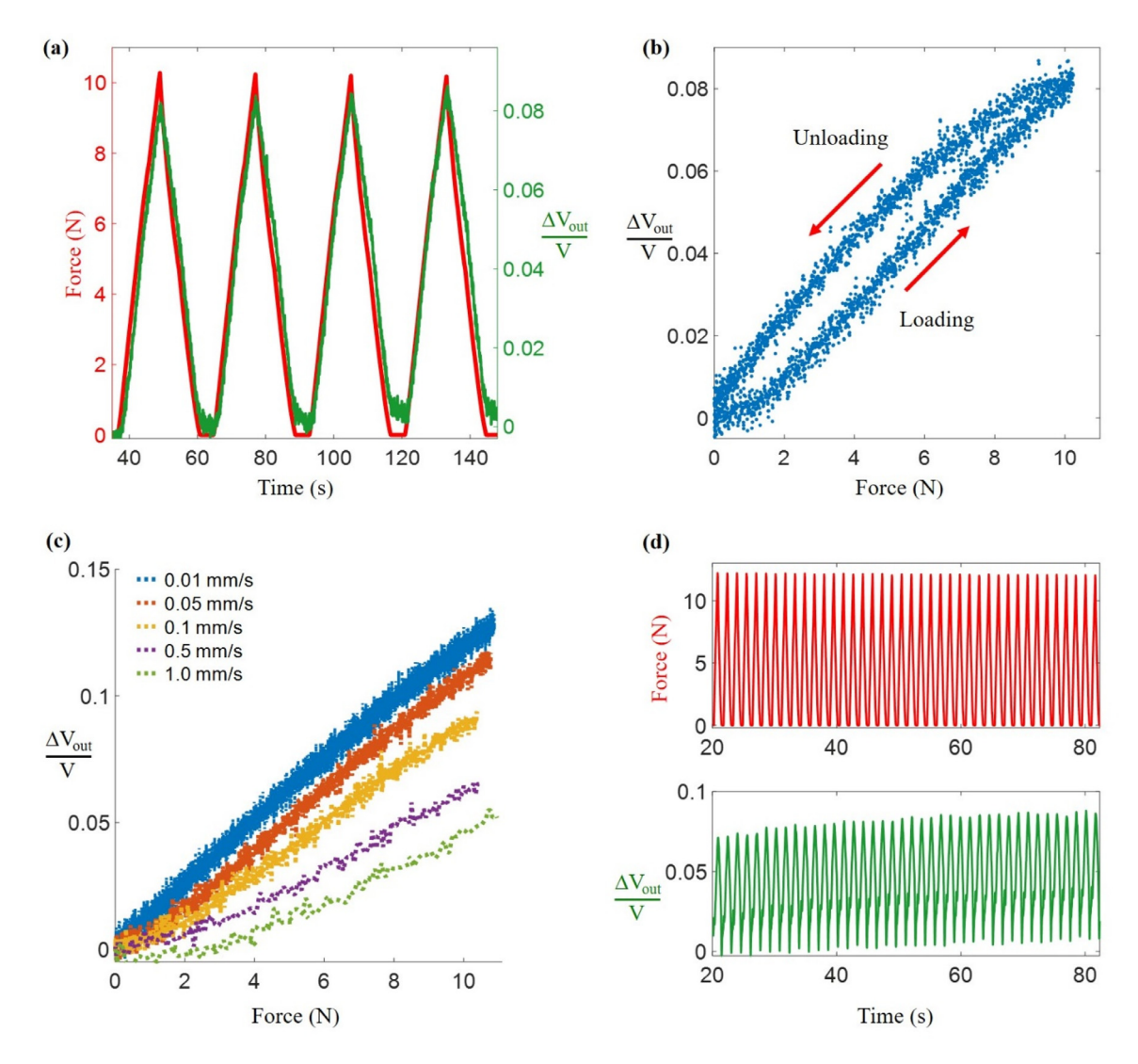


Fig. 8. Conformally printed sensor evaluation: (a) applied force (in red) and sensor output (in green); (b) hysteresis curve for the sensor; (c) sensor output for different strain rates (probe speeds); and (d) sensor signal and applied force after the sensor was subjected to hundreds of cycles.

loading delay depends on the applied strain rate where higher strain rates result in longer delay and smaller rates result in shorter delay. The difference between loading and unloading, shown in the hysteresis curve for the four cycles shown in Fig. 8(b), occurs due to the energy loss in a cycle, which is a common viscoelastic property of the soft elastomer [33,34]. The sensor was also tested at different probe speeds or strain rates. Fig. 8(c) shows the sensor output with force for varying probe speeds. As can be noticed from this figure, the sensor shows a higher sensitivity at a lower strain rate. Fig. 8(d) shows the reliability of the sensor signal after the sensor had undergone a few hundred cycles of applied force at a probe speed of 1 mm/s.

3.3. Comparison of planar and conformally printed sensors

Planar 3D printing and conformal 3D printing of sensors were conducted on a flat surface and a curved surface, respectively, using the same geometry and printing parameters. First, flat and curved sensors were designed to have the same overall dimensions with the only difference in the curvature of the sensor for conformal printing. Next, the flat and curved sensor designs were sliced planarly and conformally, respectively, using the same printing parameters. Finally, they both were printed on the fingertip model in order to maintain a fixed mechanical property of the bottom substrate (Fig. 9(b)). The printed sensors were

photo-cured prior to testing. A compressive normal force was applied on the taxels using a 0.5 mm/s probe speed. In Fig 9(c), which presents a plot of the sensor signal versus force for planar and conformal printing, it can be seen that the overall trends for planar and conformal printing are similar. However, some differences can be observed. For the same applied force, a higher relative change in voltage was noticed in the conformally printed sensor. Also, from the hysteresis curve, it is evident that the flat sensor lost more energy than the conformally printed sensor. This difference could be attributed to factors such as the curvature in the non-flat sensor and extrusion non-uniformity. In the curved sensor, the strain propagation could vary due to the concaveness of the taxel, which may induce higher strain in the IL-based layer of the curved sensor as compared to that in the IL-based layer of the flat sensor.

4. Discussion

As reported in the results in Section 3, conformal slicing and 3D printing of functional polymer composites were successfully conducted for structures printed on curved fixtures. These structures are difficult or, in some cases, unfeasible to print via planar printing. The conformal process not only successfully printed the curved parts, but the parts also retained their functionality. Fig. 6 shows how flat and conformally printed CNT/polymer composites have similar dimensions and electri-

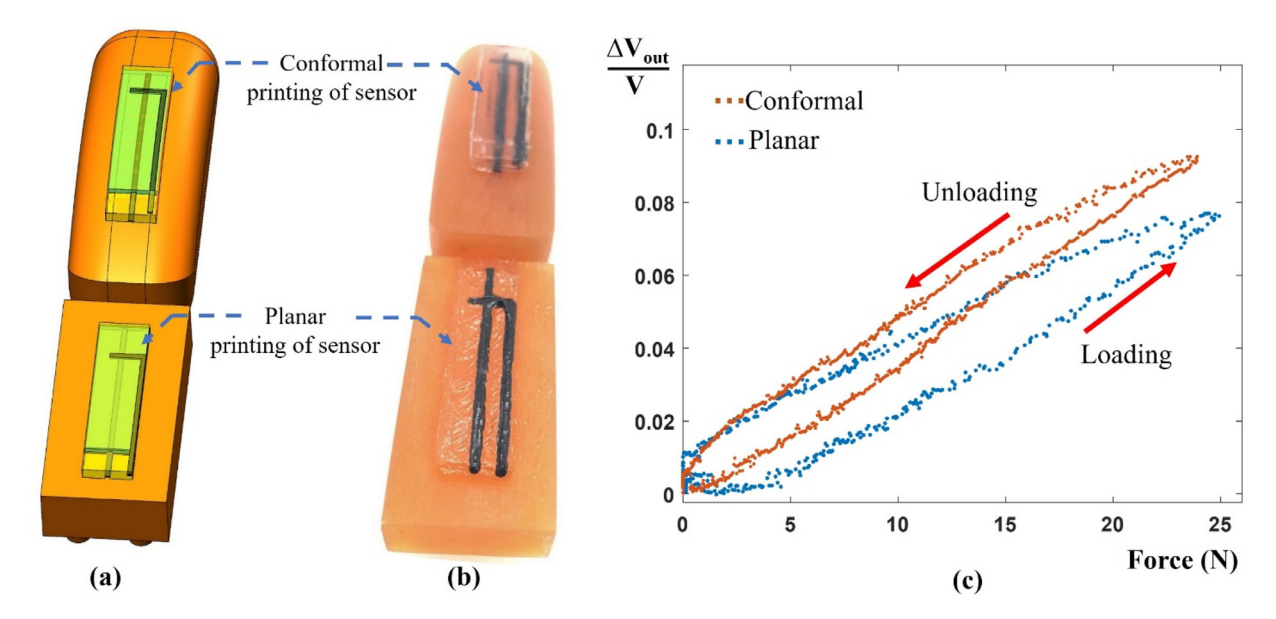


Fig. 9. Comparison of sensors fabricated through planar and conformal 3D printing: (a) schematic of sensors printed on flat and curved surfaces; (b) photograph of the as-printed sensors; (c) sensor responses of sensors fabricated by planar printing and conformal printing.

cal properties. The soft polymeric pressure sensor was also conformally sliced and printed on a curved fingertip. The multi-material direct-print system employed a photopolymerization technique using UV light to cure the printed layers.

A few challenges were encountered in the printing process in terms of homing the extrusion nozzle and stopping extrusion immediately upon command. However, these are solvable issues. In this study, only one camera was used to home the print nozzle with respect to the sharp conical post in the reference base. As this camera only provides a twodimensional view, some position errors were noticed during the printing of the sensor. In future studies, multiple cameras could be used to resolve the homing errors. Another issue was the generation of a bulge at the end of a printed line. At the beginning of a print, a wait time was introduced to adjust the extrusion, travel, and position. However, at the end of the print, stopping the material a little earlier than the end position did not prevent bulging. A vacuum or negative pressure in the syringe could solve the problem, as suction would pull the material back into the syringe and stop the extrusion process immediately. Unfortunately, the pressure control units used in this study were not capable of creating negative pressure. Even so, the bulge formation was not a major concern, as the bulges did not have any noticeable impact on the overall sensor structure.

The conformally printed sensor demonstrated reliable performance in various tests. The sensor has shown some hysteresis loss and a delay in the unloading signal when subjected to force cycles. However, the sensor signal or the loading/unloading trends were consistent for multiple cycles, as shown in Fig. 8(b). Hysteresis loss is common in soft elastomers because of their time-dependent elastic properties [33,34]. Also, as shown in Fig. 8(c), the sensor response depends on the strain rate. The sensitivity lessens at a higher strain rate, as it does not provide sufficient time for molecular rearrangement [35]. Finally, the conformally printed sensor showed a slightly different sensitivity as compared to the flat sensor (Fig. 9(c)), which may result from the concaveness at the taxel or the fabrication uncertainties. In addition, the applied force for the conformally printed sensor may not be fully normal. Although the fingertip model was rotated to apply normal force on the taxel, the 8° rotation brought only one point on the taxel at a horizontal plane. The taxel still had a curved surface with a small amount of concavity. This slight curvature could play a role in developing a different strain when using the same force and could subsequently result in a variation in the sensor response. Some electrical noise was noticed in the sensor signal, especially at lower strain rates (Fig. 8(c)). This could be resolved by adding signal filters. Overall, the sensor showed a reliable and consistent response under different conditions.

5. Conclusions

In this work, a soft polymeric pressure/tactile sensor was conformally 3D printed on a curved surface. Curvilinear G-code was generated for the curved sensor using a curved slicer surface. An ionic liquid (IL)-based soft pressure-sensitive polymer membrane and CNT-based conductive electrodes were conformally printed on a fingertip model. The sensor performed reliably in various tests. A comparison between conformal and planar 3D printing was also conducted. Conformal 3D printing demonstrated successful printing of functional structures, and it successfully overcame the limitations of conventional planar printing when printing on a curved surface. The work in this study is believed to pave a path for many future applications in robotics and prosthetics, where conformally printed soft sensors would provide unparalleled design freedom, customizability, and pliability.

Declaration of Competing interest

The authors declare that they have no known competing financial interests or personal relationships that could have appeared to influence the work reported in this paper.

Acknowledgments

This work was supported by research grants from the Center for Tire Research.

Supplementary materials

Supplementary material associated with this article can be found, in the online version, at doi:10.1016/j.addlet.2022.100027.

References

 B.E. Kelly, I. Bhattacharya, H. Heidari, M. Shusteff, C.M. Spadaccini, H.K. Taylor, Volumetric additive manufacturing via tomographic reconstruction, Science 363 (2019) 1075–1079, doi:10.1126/science.aau7114.

- [2] F. Alkadi, K.-C. Lee, A.H. Bashiri, J.-W. Choi, Conformal additive manufacturing using a direct-print process, Addit. Manuf. 32 (2020) 100975, doi:10.1016/j.addma.2019.100975.
- [3] L.-Y. Zhou, J. Fu, Y. He, A review of 3D printing technologies for soft polymer materials. Adv. Funct. Mater. 30 (2020) 2000187. doi:10.1002/adfm.202000187
- [4] I. Cooperstein, E. Sachyani-Keneth, E. Shukrun-Farrell, T. Rosental, X. Wang, A. Kamyshny, S. Magdassi, Hybrid materials for functional 3D printing, Adv. Mater.Interfaces 5 (2018) 1800996, doi:10.1002/admi.201800996.
- [5] G. Palmara, F. Frascella, I. Roppolo, A. Chiappone, A. Chiadò, Functional 3D printing: approaches and bioapplications, Biosens. Bioelect. 175 (2021) 112849, doi:10.1016/j.bios.2020.112849.
- [6] X.-Y. Yin, Y. Zhang, X. Cai, Q. Guo, J. Yang, Z.L. Wang, 3D printing of ionic conductors for high-sensitivity wearable sensors, Mater. Horiz. 6 (2019) 767–780, doi:10.1039/C8MH01398F.
- [7] R.L. Truby, M. Wehner, A.K. Grosskopf, D.M. Vogt, S.G.M. Uzel, R.J. Wood, J.A. Lewis, Soft somatosensitive actuators via embedded 3D printing, Adv. Mater. 30 (2018) 1706383, doi:10.1002/adma.201706383.
- [8] E. Sachyani Keneth, A. Kamyshny, M. Totaro, L. Beccai, S. Magdassi, 3D printing materials for soft robotics, Adv. Mater. 33 (2021) 2003387, doi:10.1002/adma.202003387.
- [9] R. Miura, T. Sekine, Y.-F. Wang, J. Hong, Y. Watanabe, K. Ito, Y. Shouji, Y. Takeda, D. Kumaki, F.D.D. Santos, A. Miyabo, S. Tokito, Printed soft sensor with passivation layers for the detection of object slippage by a robotic gripper, Micromachines (Basel) 927 (11) (2020), doi:10.3390/mil1100927.
- [10] R.P. Rocha, P.A. Lopes, A.T. de Almeida, M. Tavakoli, C. Majidi, Fabrication and characterization of bending and pressure sensors for a soft prosthetic hand, J. Micromech. Microeng. 28 (2018) 034001, doi:10.1088/1361-6439/aaa1d8.
- [11] D. Singh, C. Tawk, R. Mutlu, E. Sariyildiz, V. Sencadas, G. Alici, A 3D printed soft force sensor for soft haptics, in: 3rd IEEE International Conference on Soft Robotics (RoboSoft), 2020, pp. 458–463, doi:10.1109/RoboSoft48309.2020.9115991.
- [12] G. Wolterink, P. Dias, R. Sanders, F. Muijzer, B.-J. van Beijnum, P. Veltink, G. Krijnen, 3D-printing soft sEMG sensing structures using 3D-printing technologies, Sens. 20 (2020) 4292, doi:10.3390/s20154292.
- [13] Z. Zhu, H.S. Park, M.C. McAlpine, 3D printed deformable sensors, Sci. Adv. 6 (2020) eaba5575, doi:10.1126/sciadv.aba5575.
- [14] L.-W. Lo, H. Shi, H. Wan, Z. Xu, X. Tan, C. Wang, Inkjet-printed soft resistive pressure sensor patch for wearable electronics applications, Adv. Mater. Technol. 5 (2020) 1900717, doi:10.1002/admt.201900717.
- [15] M.O.F. Emon, A. Russell, G. Nadkarni, J.-W. Choi, A low-cost visual grasp aid for neuropathy patients using flexible three-dimensional printed tactile sensors, J. Med.Device. 15 (2021) 034502, doi:10.1115/1.4051247.
- [16] Y. Xia, H. Gu, L. Xu, X.D. Chen, T.V. Kirk, Extending porous silicone capacitive pressure sensor applications into athletic and physiological monitoring, Sens. 21 (2021) 1119, doi:10.3390/s21041119.
- [17] M.O.F. Emon, F. Alkadi, D.G. Philip, D.-H. Kim, K.-C. Lee, J.-W. Choi, Multi-material 3D printing of a soft pressure sensor, Addit. Manuf. 28 (2019) 629–638, doi:10.1016/j.addma.2019.06.001.
- [18] M. Seo, S. Hwang, T. Hwang, J. Yeo, Fabrication of soft sensor using laser processing techniques: for the alternative 3D printing process, Materials (Basel) 12 (2019) 2955, doi:10.3390/ma12182955.
- [19] E. Jabari, F. Liravi, E. Davoodi, L. Lin, E. Toyserkani, High speed 3D material-jetting additive manufacturing of viscous graphene-based ink with high electrical conductivity, Addit. Manuf. 35 (2020) 101330, doi:10.1016/j.addma.2020.101330.

- [20] G. Zeb, S. Young, C. Hyun, Fully 3D printed multi-material soft bio-inspired whisker sensor for underwater-induced vortex detection, Soft Robot. 5 (2018) 122–132, doi:10.1089/soro.2016.0069.
- [21] M.O.F. Emon, J.-W. Choi, Flexible piezoresistive sensors embedded in 3D printed tires. Sensors 17 (2017) 656. doi:10.3390/s17030656.
- [22] M.O.F. Emon, J.-W. Choi, A preliminary study on 3D printed smart insoles with stretchable piezoresistive sensors for plantar pressure monitoring, ASME 2017 Intern. Mechan. Engin. Congress and Exposition (2018), doi:10.1115/IMECE2017-71817.
- [23] Y. Khan, A. Thielens, S. Muin, J. Ting, C. Baumbauer, A.C. Arias, A new frontier of printed electronics: flexible hybrid electronics, Adv. Mater. 32 (2020) 1905279, doi:10.1002/adma.201905279.
- [24] H. Yuk, B. Lu, S. Lin, K. Qu, J. Xu, J. Luo, X. Zhao, 3D printing of conducting polymers, Nat. Commun. 11 (2020) 1604, doi:10.1038/s41467-020-15316-7.
- [25] J. Lee, M.O.F. Emon, M. Vatani, J.-W. Choi, Effect of degree of crosslinking and polymerization of 3D printable polymer/ionic liquid composites on performance of stretchable piezoresistive sensors, Smart Mater. Struct. 26 (2017) 035043, doi:10.1088/1361-665X/aa5c70.
- [26] K.S. Ramadan, D. Sameoto, S. Evoy, A review of piezoelectric polymers as functional materials for electromechanical transducers, Smart Mater. Struct. 23 (2014) 033001, doi:10.1088/0964-1726/23/3/033001.
- [27] Y.M. Almazrou, H.A. Albehaijan, J. Jeong, T. Kyu, Flexoelectricity of multifunctional polymer electrolyte membranes: effect of polymer network functionality, ACS Appl. Energy Mater. 4 (2021), doi:10.1021/acsaem.1c02459.
- [28] J.H. Kim, S. Lee, M. Wajahat, H. Jeong, W.S. Chang, H.J. Jeong, J.-R. Yang, J.T. Kim, S.K. Seol, Three-dimensional printing of highly conductive carbon nanotube microarchitectures with fluid ink, ACS Nano 10 (2016) 8879–8887, doi:10.1021/acsnano.6b04771.
- [29] Mora, A., Verma, P., Kumar, S., 2020. Electrical conductivity of CNT/polymer composites: 3D printing, measurements and modeling, compos. B: eng. 183, 107600. doi:10.1016/j.compositesb.2019.107600.
- [30] M.O.F. Emon, J. Lee, U.H. Choi, D.-H. Kim, K.-C. Lee, J.-W. Choi, Characterization of a soft pressure sensor on the basis of ionic liquid concentration and thickness of the piezoresistive layer, IEEE Sens. J. 19 (2019) 6076–6084, doi:10.1109/JSEN.2019.2911859.
- [31] D.M. Correia, L.C. Fernandes, P.M. Martins, C. García-Astrain, C.M. Costa, J. Reguera, S. Lanceros-Méndez, Ionic liquid-polymer composites: a new platform for multifunctional applications, Adv. Funct. Mater. 30 (2020) 1909736, doi:10.1002/adfm.201909736.
- [32] H. Nulwala, A. Mirjafari, X. Zhou, Ionic liquids and poly(ionic liquid)s for 3D printing – A focused mini-review, Eur Polym J 108 (2018) 309–398, doi:10.1016/j.eurpolymj.2018.09.023.
- [33] N.W. Tschoegl, Time dependence in material properties: an overview, Mech. Time Depend.Mater. 1 (1997) 3–31, doi:10.1023/A:1009748023394.
- [34] L. Qiu, M. Bulut Coskun, Y. Tang, J.Z. Liu, T. Alan, J. Ding, V.-T. Truong, D. Li, Ultrafast dynamic piezoresistive response of graphene-based cellular elastomers, Adv. Mater. 28 (2016) 194–200, doi:10.1002/adma.201503957.
- [35] V. Slesarenko, S. Rudykh, Towards mechanical characterization of soft digital materials for multimaterial 3D-printing, Int. J. Eng. Sci. 123 (2018) 62–72, doi:10.1016/j.ijengsci.2017.11.011.